Cancer Research

Epigenetic Regulator Smchd1 Functions as a Tumor Suppressor

Huei San Leong[1,2], Kelan Chen[1,2], Yifang Hu[1], Stanley Lee[1,2], Jason Corbin[1], Miha Pakusch[1], James M. Murphy[1,2], Ian J. Majewski[5], Gordon K. Smyth[1,3], Warren S. Alexander[1,2], Douglas J. Hilton[1,2], and Marnie E. Blewitt[1,2,4]

Abstract

SMCHD1 is an epigenetic modifier of gene expression that is critical to maintain X chromosome inactivation. Here, we show in mouse that genetic inactivation of *Smchd1* accelerates tumorigenesis in male mice. Loss of Smchd1 in transformed mouse embryonic fibroblasts increased tumor growth upon transplantation into immunodeficient nude mice. In addition, loss of Smchd1 in Eμ-*Myc* transgenic mice that undergo lymphomagenesis reduced disease latency by 50% relative to control animals. In premalignant Eμ-*Myc* transgenic mice deficient in Smchd1, there was an increase in the number of pre-B cells in the periphery, likely accounting for the accelerated disease in these animals. Global gene expression profiling suggested that Smchd1 normally represses genes activated by MLL chimeric fusion proteins in leukemia, implying that Smchd1 loss may work through the same pathways as overexpressed MLL fusion proteins do in leukemia and lymphoma. Notably, we found that *SMCHD1* is underexpressed in many types of human hematopoietic malignancy. Together, our observations collectively highlight a hitherto uncharacterized role for SMCHD1 as a candidate tumor suppressor gene in hematopoietic cancers. *Cancer Res; 73(5); 1591–9.* ©*2012 AACR.*

Introduction

Smchd1 was originally identified as a regulator of the epigenetic silencing of transgenes and metastable epialleles in mice (1). An ENU-induced point mutation, termed *MommeD1* (*MD1*), results in nonsense-mediated mRNA decay, effectively producing a null allele of *Smchd1*. *Smchd1*$^{MD1/MD1}$ female embryos die in mid-gestation by embryonic day 10.5 (E10.5), whereas homozygous males are unaffected at this time. These observations were confirmed using a genetrap allele of Smchd1 (*Smchd1*^{gt}), which also behaves as a null allele (2). Female-specific embryonic lethality is due to the critical role that Smchd1 plays in X chromosome inactivation, where Smchd1 is required for DNA methylation and silencing of genes on the inactive X chromosome and appears to be involved in the maintenance of X chromosome inactivation (2). Notably, only half of *Smchd1*$^{MD1/MD1}$ males survive to weaning (1), suggesting that Smchd1 has additional roles, consistent with its function in silencing autosomal transgenes and metastable epialleles.

Smchd1 encodes a 2007 amino acid protein with an N-terminal ATP-binding domain and a conserved C-terminal SMC hinge domain. SMC hinge domains are otherwise found in the 6 canonical SMC family members, where a central hinge domain mediates DNA binding and heterodimerization between SMC proteins to form 3 distinct complexes involved in chromosome condensation, cohesion, and DNA repair (3).

Many epigenetic regulators are aberrantly expressed or somatically mutated in diverse human cancers (4), so we were interested to test whether Smchd1 played a role in malignancy. Because of embryonic lethality of *Smchd1*-null females, we restricted our analyses to male mice. We show that loss of Smchd1 enhances growth in a fibroblast transformation model and accelerates development of Eμ-*Myc* B-cell lymphoma, showing that Smchd1 acts as a tumor suppressor.

Materials and Methods

Mouse strains

Mice with mutations in *Smchd1* (MommeD1 and genetrap alleles) were previously described (2). The *Smchd1*^{MD1} mice were maintained on the FVB/N background, and *Smchd1*^{gt} mice were backcrossed with C57BL/6 mice for more than 10 generations. The Eμ-*Myc* transgenic mice were described previously (5) and are congenic with C57BL/6. All genotyping was as previously described (2, 6). All mice were housed under specific pathogen-free (SPF) conditions, under the approval of

Authors' Affiliations: [1]The Walter and Eliza Hall Institute of Medical Research, Parkville; Departments of [2]Medical Biology, [3]Mathematics and Statistics, and [4]Genetics, University of Melbourne, Carlton, Victoria, Australia; and [5]The Netherlands Cancer Institute, Amsterdam, The Netherlands.

Note: Supplementary data for this article are available at Cancer Research Online (http://cancerres.aacrjournals.org/).

Corresponding Author: Marnie E. Blewitt, The Walter and Eliza Hall Institute of Medical Research, 1G Royal Pde, Parkville 3052 VIC, Australia. Phone: 61393452545; Fax: 61393470852; E-mail: blewitt@wehi.edu.au

doi: 10.1158/0008-5472.CAN-12-3019

the Walter and Eliza Hall Institute of Medical Research Animal Ethics Committee (VIC, Australia).

Mouse embryonic fibroblast culture and transformation

Primary mouse embryonic fibroblasts (MEF) were generated from E13.5 embryos by passing the embryonic body (excluding head, liver, and intestines) through a 21-gauge syringe then repeated pipetting and cultured in Dulbecco's Modified Eagle's Medium (DMEM) containing 10% (v/v) fetal calf serum (FCS; Gibco, Invitrogen). Retroviral supernatants were prepared as previously described (7). The LMP-p53.1224 shRNA and pWZL-Hras^{V12} cDNA constructs were provided by Dr. R.A. Dickins (Walter and Eliza Hall Institute) and have been previously described (8, 9). Early-passage (p1–4) MEFs were seeded 24 hours before transduction. MEFs were cocultured with the retrovirus in the presence of 4 μg/mL hexadimethrine bromide (polybrene, Sigma) at 37°C overnight, 10% CO_2. Transduction was repeated the following day. MEFs transduced with LMP-p53.1224 short hairpin RNA (shRNA) retrovirus were selected in puromycin (5 μg/mL; Sigma) for 2 days, transduced with pWZL-Hras^{V12} retrovirus, and selected in hygromycin (300 μg/mL; Invitrogen) for 6 days. MEFs were then passaged for at least 2 weeks to remove senescent cells that do not contribute to tumor growth.

In vivo tumor growth in immunodeficient nude mice

A total of 1×10^6 transformed MEFs were injected subcutaneously into each of the 2 rear flanks of C57BL/6 athymic nude mice aged 6 to 10 weeks. These mice were monitored daily and tumors typically arose 3 to 5 days post-injection and were measured every 2 days using a digital caliper (Mitutoyo). Tumor volumes were calculated as $\pi/6 \times \text{width}^2 \times$ length (10). Once tumors reached 10 mm in diameter, mice were culled and tumors excised for DNA, RNA, and *ex vivo* cell culture.

Design of *Smchd1* short hairpin RNAs

Short hairpin RNA (shRNA) constructs that target *Smchd1* were designed using the DSIR website (11, 12), see Supplementary Table S1 for sequence information. An shRNAmir construct containing a nonsilencing sequence was obtained from Open Biosystems (7). These shRNAs were cloned into LMP/LMS vectors that drive expression of a modified miRNA (mir30 backbone).

Hematopoietic reconstitution of lethally irradiated recipients with fetal liver cells

E14.5 fetal liver cells from *Smchd1*$^{+/+}$/Eμ-*Myc*$^{Tg/+}$ or *Smchd1*$^{gt/gt}$/Eμ-*Myc*$^{Tg/+}$ male embryos (C57BL/6 *CD45*$^{Ly5.2}$) were used to reconstitute lethally irradiated (2×550 Rads in a 3-hour interval) *CD45*$^{Ly5.1}$ recipients. Single-cell suspensions were prepared in KDS BSS (150 mmol/L NaCl, 3.7 mmol/L KCl, 2.5 mmol/L $CaCl_2$, 1.2 mmol/L $MgSO_4$, 7.4 mmol/L HEPES. NaOH, 1.2 mmol/L KH_2PO_4, 0.8 mmol/L K_2HPO_4) supplemented with 5% FCS. A total of 1×10^6 nucleated fetal liver cells were mixed with 0.2×10^6 *CD45*$^{Ly5.1}$-nucleated bone marrow cells for intravenous tail vein injection into recipient mice. Recipient mice were maintained on neomycin sulfate-supplemented drinking water for 21 days after radiation to prevent infection.

Hematopoietic analysis of premalignant phenotype in reconstituted Eμ-*Myc*$^{Tg/+}$ mice

Blood was obtained from live Eμ-*Myc* transgenic mice via the retro-orbital sinus at 8 weeks posttransplant to monitor their white blood cell numbers. Hematologic analysis was conducted using an ADVIA hematology system (Bayer). Single-cell suspensions were prepared from the bone marrow by flushing from both femurs and for bone marrow, spleen, and thymus, by filtering through a 100-μm cell strainer. The remainder of the blood, along with bone marrow and spleen cells, was treated with red cell lysis buffer (156 mmol/L NH_4Cl, 0.1 mmol/L EDTA, 12 mmol/L $NaHCO_3$) for 5 minutes at room temperature and resuspended in 5% KDS BSS-FCS before staining with monoclonal antibodies and subsequent flow cytometric analysis (below). Total numbers of cell type were calculated by multiplying the total cellularity (hemocytometer counts) by the percentage of cells of that type as determined by flow cytometry.

Flow cytometric analysis and cell sorting

Cells were stained for at least 30 minutes on ice with monoclonal antibodies (BD Biosciences) specific to cell surface proteins of interest conjugated to fluorescein isothiocyanate, phycoerythrin (PE), allophycocyanin, peridinin chlorophyll A protein, or biotin. Commonly used monoclonal antibodies were against *CD45*$^{Ly5.2}$ (clone 104), progenitor marker c-kit (2B8), and B-cell surface markers B220 (clone RA3-6B2), IgM (clone II/41), and IgD (clone 11-26C.2a). Cells were washed with 5% KDS BSS-FCS and resuspended in 5% KDS BSS-FCS with 1 μg/mL propidium iodide (Sigma) or 2.5 μg/mL fluorogold (Molecular Probes), to allow exclusion of dead cells. Samples were run on either an LSR I or II flow cytometer (BD Biosciences) for analysis and on a MoFlo (Beckman Coulter), FACSDiva (BD Biosciences), or FACSAria (BD Biosciences) for cell sorting. Results were analyzed using FlowJo software (Treestar Inc.).

In vitro limiting dilution assays

Pro-B cells [Ly5.2$^+$ (for transplant recipients) B220$^+$c-kit$^+$IgM$^-$] were fluorescence-activated cells sorter (FACS)-purified from reconstituted animals at 8 weeks posttransplant (*Smchd1*^{gt} allele) or at 7 to 8 weeks of age (*Smchd1*^{MD1} allele). Four thousand OP-9 cells were seeded in each well of 96-well plate on the day of experiment. Two hundred pro-B cells were seeded onto OP-9 stromal cells, in the presence of interleukin (IL)-7, in 12 to 16 wells of 96-well plate, and serially diluted 1 in 2 until ~1 cell per well was reached. The number of wells with colonies was scored after 7 days in culture. Data are shown as $\log_{10}$ fraction of negative wells. OP-9 cells were cultured in α-MEM medium (Gibco GlutaMAX 32561) supplemented with 20% FCS, 100 U/mL penicillin, 100 μg/mL streptomycin, 10 mmol/L HEPES (Gibco BRL), and 1 mmol/L sodium pyruvate (Gibco BRL). Pro-B cells were cultured in the same medium except 10% FCS and further supplemented with 2% IL-7 supernatant.

RNA extraction

RNA was extracted using an RNeasy Mini Kit (Qiagen), according to the manufacturer's instructions. RNA quantity and purity were determined using the NanoDrop 1000 Spectrophotometer (Thermo Scientific) and stored at −80°C.

Microarray analysis

RNA quality was ascertained with the Agilent Bioanalyzer 2100 (Agilent Technologies) using the Agilent 600 NanoChip (Agilent Technologies) according to the manufacturer's protocol. Either 2 μg (MEFs and tumors from nude mice) or 150 ng (purified Eμ-*Myc* pre-B cells or lymphoma cells) of RNA was labeled, amplified, and hybridized to Illumina MouseWG-6 V2.0 Expression BeadChips (Illumina) according to Illumina standard protocols at the Australian Genome Research Facility.

Unnormalized summary probe profiles were exported from GenomeStudio for analysis using the limma package of the Bioconductor software project (13). Probe annotation from the Illumina manifest file was used except that gene symbols were updated to the latest official symbols using the Bioconductor annotation package org.Mm.eg.db. Data on each cell type (primary MEFs, transformed MEFs, nude tumors, E17.5 pre-B cells, premalignant pre-B cells, and B-cell lymphomas) were analyzed separately. Probes intensities were normexp background corrected and quantile-normalized using control probes (14). Probes were filtered as unexpressed if they failed to achieve a detection P of 0.05 in at least n arrays, where n is the number of arrays for each genotype or tumor ($n = 3$ or 6 depending on the cell type). Differential expression between the *Smchd1* null and wild-type samples was assessed using linear models and empirical Bayes-moderated t statistics (15). Batch effects for different Illumina bead chips were included as appropriate. Empirical quality weights were estimated as appropriate to allow for variable sample quality (16). The recipient nude tumor mice that were injected from the same MEF line were treated as a random block allowing for correlation between the replicates (17). The false discovery rate was controlled at 5% (18). Pathway analysis used the "camera" competitive gene set test methodology to allow for correlation between genes (19). Camera was applied to the C2 collection of curated gene sets of the Molecular Signatures Database (MSigDB) v3 (20). A pure mouse version of the MSigDBin was created by mapping human to mouse gene symbols using Jackson Laboratory ortholog tables (21) and software is available (22). Array data are available on Gene Expression Omnibus (GEO; accession number GSE40992).

Statistical analysis

The permutation tests conducted on the tumor volumes used the "compareGrowthCurves" function of the "statmod" software package for the R computing environment (23) as described (24). Prism software (GraphPad Software Inc.) was used to conduct 1- or 2-tailed t tests and log-rank tests (for Kaplan–Meier survival curves). The limiting dilution assays were analyzed using the extreme limiting dilution software as previously described (25).

Results and Discussion

Loss of Smchd1 alone is not oncogenic

Approximately half of *Smchd1*$^{MD1/MD1}$ male mice survived to weaning (1); however, they were not predisposed to spontaneous tumor formation as adults, even when aged up to 2 years ($n > 20$, data not shown). This suggests that lack of Smchd1 is not inherently oncogenic.

We next tested whether loss of Smchd1 can transform immortalized cells. We derived primary MEFs from E13.5 *Smchd1*$^{+/+}$, *Smchd1*$^{MD1/+}$, and *Smchd1*$^{MD1/MD1}$ male embryos and immortalized these cells with a retrovirus carrying an shRNA to reduce expression of *p53* (9). To evaluate the tumorigenic potential of these cells, we injected 1 million cells subcutaneously into each of the 2 rear flanks of immunodeficient nude mice. Immortalized *Smchd1*-null MEFs did not form tumors in nude mice even when monitored for 5 months following injection (data not shown), again suggesting that loss of Smchd1 is not a transforming event. Therefore, we investigated the effect of Smchd1 deficiency in 2 oncogene-driven tumor models.

Smchd1 deficiency in transformed fibroblasts led to accelerated tumor growth in immunodeficient nude mice

Immortalized *Smchd1*$^{+/+}$, *Smchd1*$^{MD1/+}$, and *Smchd1*$^{MD1/MD1}$ male MEFs were generated as above, transformed with the H-Ras^{V12} oncogene (8), and injected into nude mice. Tumors were measured every 2 days using a digital caliper. No significant difference in tumor growth was observed in recipients of *Smchd1*$^{MD1/+}$ and *Smchd1*$^{+/+}$ cells, suggesting that Smchd1 is not haploinsufficient in this context. In contrast, mice injected with *Smchd1*$^{MD1/MD1}$ MEFs reached maximum tumor size (>10 mm in any dimension) more rapidly than animals that received *Smchd1*$^{MD1/+}$ or *Smchd1*$^{+/+}$ cells (Fig. 1A). To verify that the tumor cells were malignant, we injected fixed numbers of *ex vivo* cultured primary tumor cells into secondary recipient mice and again showed accelerated growth in *Smchd1*$^{MD1/MD1}$ cells compared with *Smchd1*$^{+/+}$ cells (Fig. 1B).

To confirm our findings, we used shRNA-mediated knockdown of *Smchd1* in primary MEFs. We used 2 hairpins that both stably reduce the expression of Smchd1 protein, determined by Western blotting, but that reduce *Smchd1* RNA to subtly different levels, as measured by quantitative reverse transcriptase (qRT)-PCR. (Supplementary Fig. S1). As Western blotting is a nonquantitative technique, we relied on the qPCR results to show the slightly different efficiency of each shRNA. These *Smchd1* shRNAs and a nonsilencing control were used to transduce E13.5 primary MEFs before immortalization and transformation as described above. Both *Smchd1* shRNAs produced accelerated tumor growth in nude mice over the first 14 days postinjection ($P < 0.05$, Fig. 1C), recapitulating the enhanced oncogenic capacity of genetically *Smchd1* null cells. At later time points, only the *Smchd1* 1.2 hairpin significantly enhanced tumor growth ($P < 0.05$, Fig. 1C), potentially due to subtle differences in the amount of Smchd1 and reflecting a dosage effect of Smchd1 in this assay where heterozygous loss of Smchd1 has no effect (Fig. 1A) and genetically null cells show the most marked effect on tumor growth. Both our genetic and

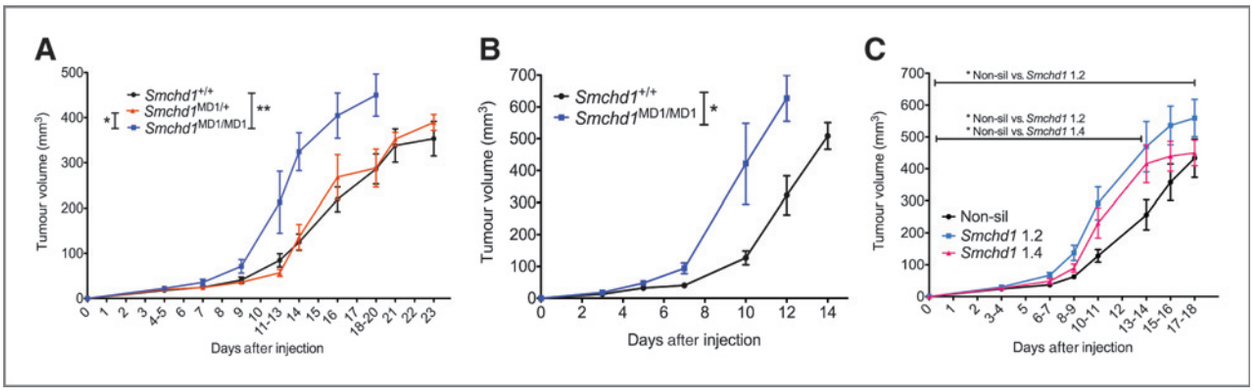

Figure 1. Smchd1 deficiency leads to increased growth in transformed fibroblast tumors. Tumor volumes of athymic nude mice injected with transformed *Smchd1*$^{+/+}$, *Smchd1*$^{MD1/+}$, or *Smchd1*$^{MD1/MD1}$ male MEFs ($n = 4$–8 embryos per genotype, 6 replicate injections per original embryo; A); secondary recipients of *ex vivo* cultured tumor cell lines ($n = 3$ independent MEF lines per genotype; B) derived from primary recipients; and nude mice injected with transformed *Smchd1* knockdown or nonsilencing male MEFs ($n = 8$ embryos per construct; C). A–C, data represent mean ± SEM of biologic replicates from 2 to 4 independent experiments (*, $P < 0.05$; **, $P < 0.01$).

knockdown data are consistent with Smchd1 acting as a tumor suppressor in transformed fibroblasts in a dose-dependent manner.

Loss of Smchd1 accelerates Eμ-*Myc*–driven B-cell lymphomas

In the Eμ-*Myc*--driven B-cell lymphoma model of Burkitt's lymphoma, the *Myc* oncogene is driven by the Eμ heavy chain enhancer, which results in progenitor (pro)/precursor (pre)-B or immature/mature B-cell lymphomas (5). We chose this model as it better recapitulates human disease than the fibroblast transformation model and because Smchd1 is particularly highly expressed in B cells (refs. 26, 27 and data not shown). We first tested whether heterozygosity for *Smchd1* altered the median tumor latency in Eμ-*Myc* transgenic mice; there was no significant difference in the median survival between *Smchd1*$^{+/+}$/Eμ-*Myc*$^{Tg/+}$ and *Smchd1*$^{MD1/+}$/Eμ-*Myc*$^{Tg/+}$ male mice (113 vs. 106 days, median survival; FVB/C57 F1 genetic background; Supplementary Fig. S2A). A similar result was observed with our genetrap allele (C57BL/6 background; Supplementary Fig. S2B). Therefore, loss of one allele of *Smchd1* did not influence lymphomagenesis, consistent with our observations in transformed MEFs.

We next tested whether loss of both alleles of *Smchd1* altered Myc-driven lymphomagenesis. *Smchd1*$^{MD1/MD1}$ males only survive on an inbred FVB/N background, not achievable with the C57BL/6 background of the Eμ-*Myc* transgene. Therefore, we used the *Smchd1*^{gt} allele that we had on the C57BL/6 inbred background. *Smchd1*$^{gt/gt}$ male embryos die between E17.5 and weaning (Supplementary Table S2), so we transplanted fetal liver cells from E14.5 *Smchd1*$^{gt/gt}$/Eμ-*Myc*$^{Tg/+}$ or *Smchd1*$^{+/+}$/Eμ-*Myc*$^{Tg/+}$ (C57BL/6 *CD45*$^{Ly5.2/Ly5.2}$) male embryos into lethally irradiated *CD45*$^{Ly5.1/Ly5.1}$ (hereafter termed Ly5.1) recipients. We used a small number of Ly5.1 bone marrow cells along with the fetal liver cells to ensure viability of recipients following irradiation, independent of the function of *Smchd1*-null stem cells. Polymorphisms at the *CD45*^{Ly5} locus allowed discrimination between donor-derived and buffer or recipient cells. At 8 weeks posttransplant, flow cytometric analysis of the peripheral blood of all recipients showed greater than 85% contribution by fetal liver–derived cells in recipients of *Smchd1* null or wild-type cells.

Mice reconstituted with *Smchd1*$^{gt/gt}$/Eμ-*Myc*$^{Tg/+}$ cells had a median tumor latency of 126 days, half that of animals reconstituted with *Smchd1*$^{+/+}$/Eμ-*Myc*$^{Tg/+}$ cells at 256 days (Fig. 2A). Bone marrow, spleen, lymph nodes, and thymus were isolated from moribund mice and immunophenotyped by flow cytometry with monoclonal antibodies to B lineage cell surface markers (c-kit/CD117, B220, IgM, and IgD). No difference was observed in the proportion of pro/pre-B and immature/mature B-cell lymphomas between *Smchd1*-null and wild-type recipients (Supplementary Fig. S2C). Moreover, peripheral leukocyte and lymphocyte counts of moribund reconstituted *Smchd1*$^{gt/gt}$/Eμ-*Myc*$^{Tg/+}$ mice were similar to that observed in *Smchd1*$^{+/+}$/Eμ-*Myc*$^{Tg/+}$ mice (Supplementary Fig. S2D), and there was no significant difference in spleen weight or cell number (Supplementary Fig. S2E and S2F). Taken together, these results suggest that loss of Smchd1 did not appear to alter the hematologic phenotype of Eμ-*Myc* lymphomas.

One potential reason for the accelerated lymphomagenesis in the absence of Smchd1 (Fig. 2A) was increased expression of the Eμ-*Myc* transgene, as Smchd1 is involved in transgene silencing (1). However, there was no difference in *Myc* transgene expression between wild-type and Smchd1-null Eμ-*Myc* lymphomas as measured by qPCR (Supplementary Fig. S3, $P = 0.18$), suggesting that Smchd1 is playing a broader role in the disease.

To confirm that the lymphomas that arose in our cohort of reconstituted mice were malignant, 1×10^6 spleen cells from 7 *Smchd1*$^{+/+}$/Eμ-*Myc*$^{Tg/+}$ and 8 *Smchd1*$^{gt/gt}$/Eμ-*Myc*$^{Tg/+}$ lymphoma–bearing mice were injected into 2 to 3 Ly5.1 recipients each. All recipients developed lymphomas with a similar latency and within 60 days (data not shown), independent of genotype, consistent with the transplantability of Eμ-*Myc* lymphoma cells previously reported (5).

As Eμ-*Myc*$^{Tg/+}$ mice have a well-defined latency period, this allowed us to assess the impact of the loss of Smchd1 on nontransformed Eμ-*Myc*$^{Tg/+}$ B lineage cells before lymphoma

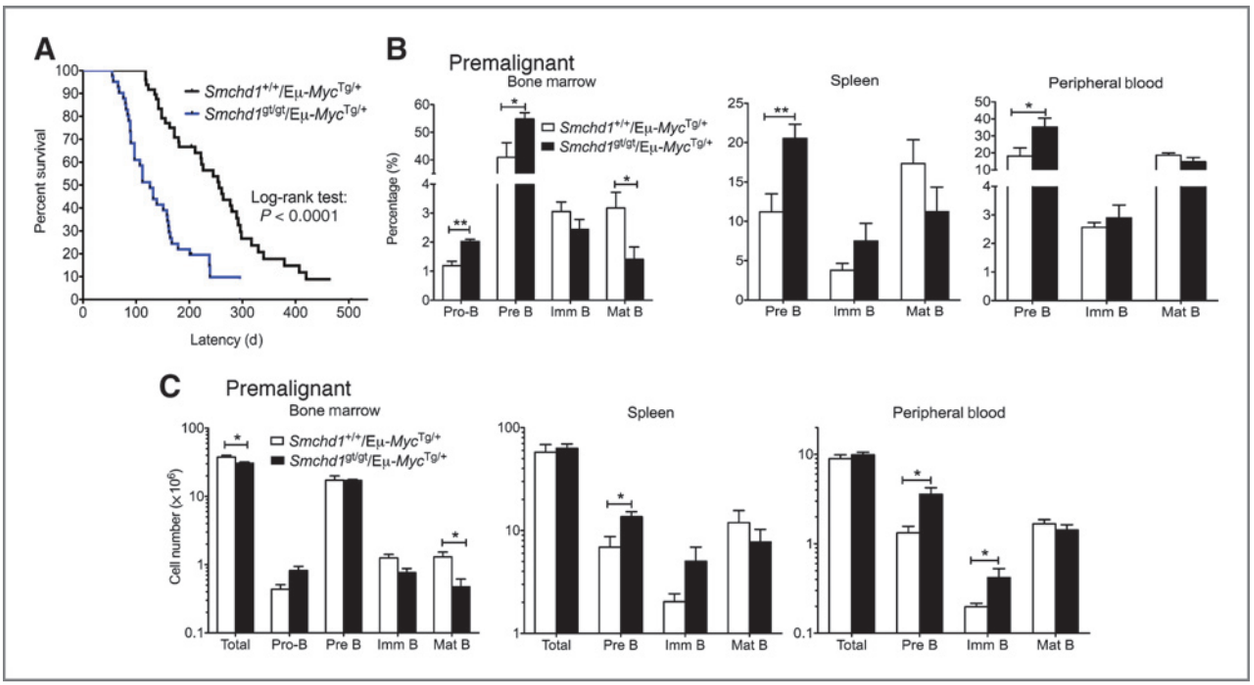

Figure 2. Smchd1 deficiency results in accelerated Eμ-*Myc*–driven lymphoma and expansion of premalignant pre-B cells. A, Kaplan–Meier survival curve of lethally irradiated mice reconstituted with fetal liver cells from *Smchd1*$^{+/+}$/Eμ-*Myc*$^{Tg/+}$ or *Smchd1*$^{gt/gt}$/Eμ-*Myc*$^{Tg/+}$ E14.5 male embryos. Median survival of reconstituted *Smchd1*$^{gt/gt}$/Eμ-*Myc*$^{Tg/+}$ and *Smchd1*$^{+/+}$/Eμ-*Myc*$^{Tg/+}$ mice was 126 and 256 days, respectively ($n = 41$–48 per genotype, $P < 0.0001$, log-rank test). B and C, peripheral blood, spleen, and bone marrow were isolated from premalignant *Smchd1*$^{+/+}$/Eμ-*Myc*$^{Tg/+}$ and *Smchd1*$^{gt/gt}$/Eμ-*Myc*$^{Tg/+}$ mice at 8 weeks posttransplant. Proportion (B) and number (C) of donor-derived pro-B, pre-B, immature B, and mature B cells were determined by cell counts and flow cytometric analysis. B and C, data represent mean and SEM of 4 to 9 mice per genotype from 2–5 independent experiments (*, $P < 0.05$; **, $P < 0.01$).

onset. Eμ-*Myc* mice have a 4- to 5-fold expansion of pre-B cells compared with their wild-type littermates starting from birth, whereas immature and mature B-cell numbers are reduced (28). Previous studies using fetal liver cells from Eμ-*Myc*$^{Tg/+}$ mice showed that between 8 and 12 weeks, posttransplantation mice were in a premalignant phase, which was verified to be lymphoma-free by secondary transplantation (28). Consistent with this, in our experiments, we have defined 8 weeks posttransplant as the premalignant stage, as secondary transplantation of 1×10^6 spleen cells into histocompatible recipients failed to produce lymphoma (2 recipients per donor, 8–9 donors, data not shown).

Analysis of premalignant Eμ-*Myc*$^{Tg/+}$ mice revealed a significant expansion in the proportion of pro-B cells by about 1.7-fold in the bone marrow, in the absence of Smchd1. Pre-B-cell frequency was also increased by about 1.4-fold in the bone marrow and about 2-fold in the spleen and peripheral blood of mice reconstituted with *Smchd1*-null cells compared with animals receiving *Smchd1* wild-type cells (Fig. 2B). In absolute terms, reconstituted *Smchd1*$^{gt/gt}$/Eμ-*Myc*$^{Tg/+}$ mice displayed a reduction in total nucleated cells in the femoral bone marrow compared with *Smchd1*$^{+/+}$/Eμ-*Myc*$^{Tg/+}$ mice (Fig. 2C), such that we only observed an increase in the absolute numbers of pre-B cells in the spleen and peripheral blood (Fig. 2C). Transplants conducted using nontransgenic fetal liver cells showed no significant differences in the reconstitution capacity of *Smchd1*-null compared with *Smchd1* wild-type cells, suggesting the hypocellularity only occurs in the context of the Eμ-*Myc* transgene (data not shown). Taken together, our data show that premalignant *Smchd1*$^{gt/gt}$/Eμ-*Myc*$^{Tg/+}$ mice exhibited a consistent and significant expansion in pre-B cells.

To assess whether loss of Smchd1 had any impact on B-cell development before birth, we measured B-cell composition in the fetal liver of E17.5 *Smchd1*-null and wild-type male embryos, with or without the Eμ-*Myc* transgene. Although we observed the expected increase in the number of pro-B and pre-B cells in all Eμ-*Myc*$^{Tg/+}$ embryos, no difference was found between *Smchd1*$^{+/+}$ and *Smchd1*$^{gt/gt}$ embryos, both those with the transgene and those without (Supplementary Fig. S4). This suggests that the B lymphoid composition of donor fetal liver cells was similar in *Smchd1*$^{+/+}$/Eμ-*Myc*$^{Tg/+}$ and *Smchd1*$^{gt/gt}$/Eμ-*Myc*$^{Tg/+}$ embryos and that differences developed following transplantation in recipient mice.

Smchd1 deficiency leads to increased clonogenicity of premalignant Eμ-*Myc* pro-B cells

To explore the cellular mechanism(s) that gave rise to elevated frequency and number of pro-B and pre-B cells in the absence of Smchd1, we first measured both proliferation and spontaneous apoptosis of pro/pre-B and immature/mature B cells isolated from bone marrow or spleen of reconstituted Eμ-*Myc*$^{Tg/+}$ mice at 8 weeks posttransplant. We found no difference in proliferation, measured using *in vivo* bromodeoxyuridine (BrdUrd) labeling, or apoptosis, measured *in vitro* by staining with Annexin V and propidium iodide (Supplementary Fig. S5).

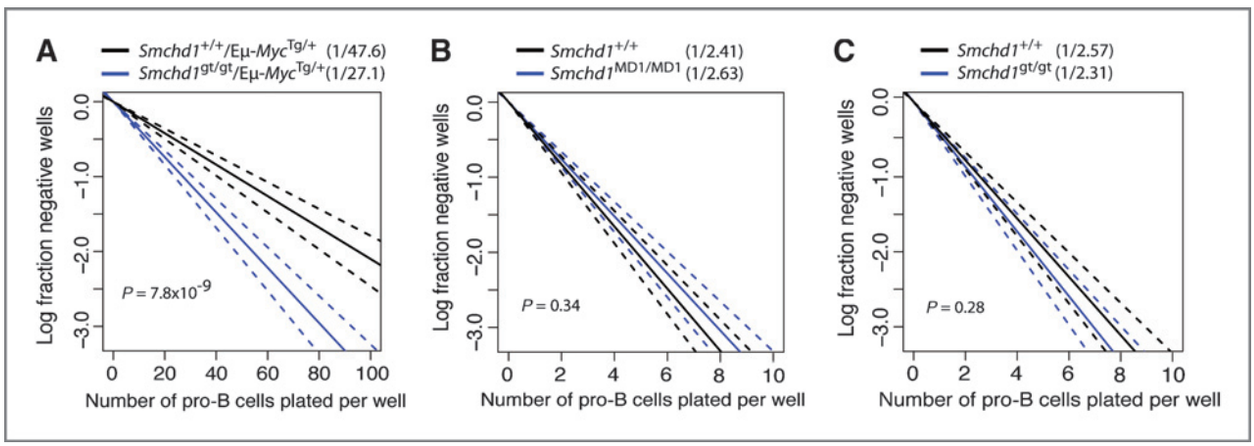

Figure 3. Loss of Smchd1 results in enhanced clonogenicity of premalignant Eμ-*Myc*$^{Tg/+}$ pro-B cells *in vitro*. A–C, data represent mean and 95% confidence intervals of 3 to 5 independent experiments. Limiting dilutions of FACS-purified pro-B cells were grown in the presence of IL-7 on an OP-9 stroma, and the proportion of wells with colonies scored after 7 days. Data are shown as $\log_{10}$ fraction of negative wells. Pro-B cells were isolated from mice reconstituted *Smchd1*$^{+/+}$/Eμ-*Myc*$^{Tg/+}$ or *Smchd1*$^{gt/gt}$/Eμ-*Myc*$^{Tg/+}$ cells at 8 weeks posttransplant ($n = 6$–8 mice per genotype, 12 technical replicates per mouse; A), giving a frequency of colony-forming pro-B cells of 1 in 47.6 and 1 in 27.1, respectively; 7-8 week-old *Smchd1*$^{+/+}$ or *Smchd1*$^{MD1/MD1}$ male mice ($n = 4$ mice per genotype, 18 technical replicates per mouse; B), giving a frequency of colony-forming pro-B cells of 1 in 2.41 and 1 in 2.63, respectively, and recipients of *Smchd1*$^{+/+}$ and *Smchd1*$^{gt/gt}$ cells at 8 weeks posttransplant ($n = 5$ mice per genotype, 12 technical replicates per mouse; C), giving a frequency of colony-forming pro-B cells of 1 in 2.57 and 1 in 2.31, respectively.

Next, we conducted *in vitro* limiting dilution assays to measure the proportion of premalignant pro-B cells with colony-forming capacity. FACS-purified pro-B cells were cultured in limiting dilutions with IL-7, on an OP-9 stroma. Consistent with the increased numbers of pre-B cells in the premalignant phase of disease, we observed increased clonogenicity in the absence of Smchd1, where twice as many *Smchd1*$^{gt/gt}$/Eμ-*Myc*$^{Tg/+}$ cells formed colonies compared with *Smchd1*$^{+/+}$/Eμ-*Myc*$^{Tg/+}$ cells (Fig. 3A).

We wanted to know whether the increased clonogenic potential observed in Eμ-*Myc*$^{Tg/+}$ cells was due to an underlying difference between wild-type and *Smchd1*-null cells. We used pro-B cells isolated from 7- to 8-week-old *Smchd1*$^{MD1/MD1}$ mice (Fig. 3B) and mice reconstituted with *Smchd1*$^{gt/gt}$ fetal liver cells at 8 weeks posttransplant (Fig. 3C). There was no difference between wild-type and Smchd1-deficient cells, using either allele, suggesting that loss of Smchd1 on its own did not enhance clonogenic capacity. Rather, we find that enhanced clonogenicity is only apparent in conjunction with Eμ-*Myc* transgene. This enhanced clonogenicity, indicating a higher B-lymphoid replicative potential, is a plausible explanation for the increase in pre-B cells and accelerated disease progression in the absence of Smchd1.

Loss of Smchd1 deregulates expression of a subset of polycomb-repressive complex 2 and mixed lineage leukemia fusion protein target genes

We used gene expression profiling to define the molecular targets and pathways potentially responsible for accelerated tumorigenesis in the absence of Smchd1 in MEFs and Eμ-*Myc*$^{Tg/+}$ hematopoietic cells. RNA was extracted from primary MEFs ($n = 3$ per genotype), transformed MEFs ($n = 3$ per genotype) and tumors derived from transformed MEFs ($n = 3$ per genotype), as well as FACS-purified Eμ-*Myc*$^{Tg/+}$ pre-B cells from E17.5 embryos ($n = 3$ per genotype), pre-B cells from premalignant mice ($n = 6$ per genotype) and B220^{+} lymphoma cells ($n = 6$ per genotype). We chose to focus on pre-B cells as this was where we observed a significant expansion in number (Fig. 2C). Samples were hybridized to Illumina whole-genome microarrays. All comparisons were made between *Smchd1*-null and wild-type samples. Pathway analysis of sets of genes enriched in the *Smchd1*-null samples was undertaken using the Camera statistical methods (19) to interrogate the Molecular Signatures Database (20).

There were few expression changes in primary MEFs and fibroblast tumors, whereas a large number of genes were differentially expressed in transformed MEFs (Fig. 4A), in part, explained by the high degree of variability between tumor samples (Supplementary Fig. S6A). *Smchd1* was consistently downregulated across the cell populations, as expected. Genes that were consistently upregulated across primary and transformed MEFs and tumors were imprinted genes, namely, *Necdin* (*Ndn*) and *Makorin3* (*Mkrn3*), and genes regulated in clusters, including *Killer cell lectin-like receptors* (*Klra*) and *Protocadherins* (*Pcdh*), which are subject to monoallelic gene expression (29, 30). These data suggest that Smchd1 is involved in regulating several different forms of monoallelic gene expression throughout the genome not just on the inactive X chromosome, and this is the subject of a separate manuscript (A. Mould, M.E. Blewitt, and G. Kay, unpublished data). As we know that loss of Smchd1 in the absence of an oncogenic driver is not sufficient for tumorigenesis (see above), this also suggests that overexpression of these genes does not contribute to the accelerated tumor growth of transformed *Smchd1*-null MEFs, consistent with the role of several of these genes in growth suppression rather than growth promotion (31, 32).

In all fibroblast populations, we observed enrichment of genesets (Supplementary Table S3) that were sensitive to

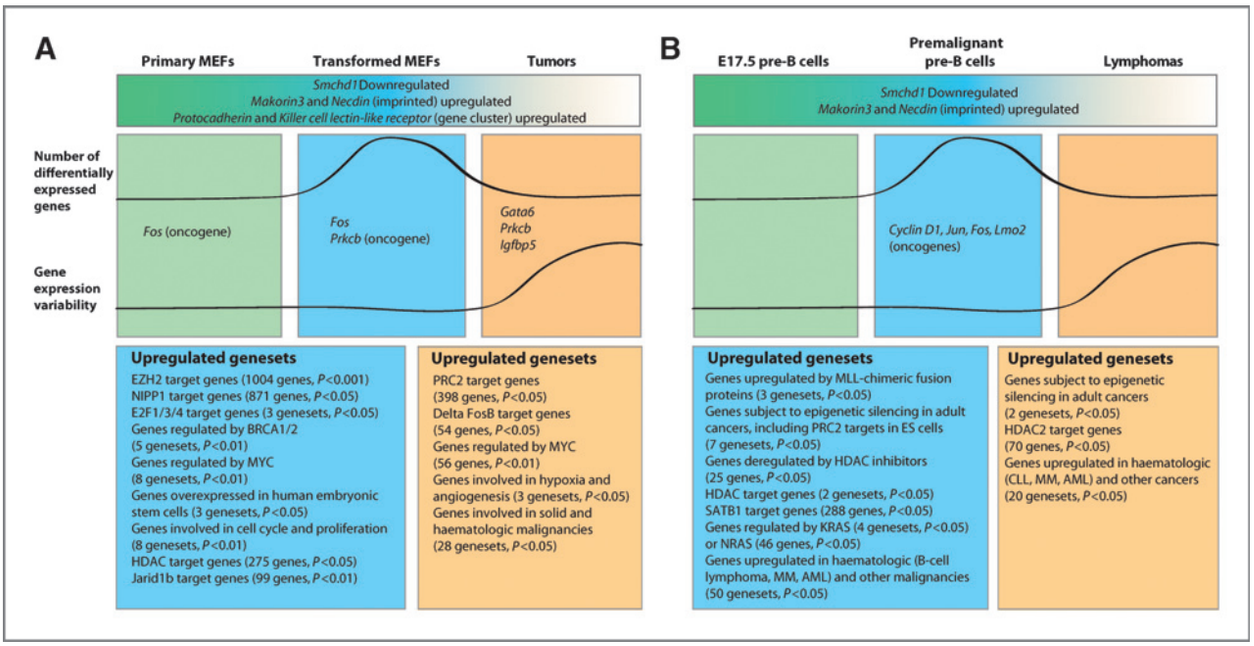

Figure 4. *Smchd1*-null MEFs and Eμ-*Myc*$^{Tg/+}$ B cells are enriched in cancer-related genesets, PRC2 target genes, and MLL fusion protein target genes. A and B, gene expression profiles of primary MEFs, transformed MEFs, and tumors isolated from nude mice (A), and E17.5 Eμ-*Myc*$^{Tg/+}$ pre-B cells, 8 weeks posttransplant premalignant Eμ-*Myc*$^{Tg/+}$ pre-B cells, and Eμ-*Myc*$^{Tg/+}$ lymphoma cells (B). Top, genes that are consistently down- and upregulated across the three stages. Middle, the relative number of differentially expressed genes and the variation in gene expression changes between cell types (shown for descriptive purposes). Genes shown in the middle are upregulated in *Smchd1*-null relative to wild-type samples. Bottom, the genesets identified in transformed MEFs or premalignant pre-B cells (blue boxes) and fibroblast tumors or Eμ-*Myc* lymphomas (orange boxes).

epigenetic control and regulation, for example, genes sensitive to histone deacetylase inhibitors (4 genesets, $P < 0.05$), consistent with the role of Smchd1 as an epigenetic repressor. In the fibroblast tumors, we observed upregulation of several cancer-associated genes including Protein kinase Cβ (*Prkcb*), Gata-binding protein 6 (*Gata6*), and insulin-like growth factor–binding protein 5 (*Igfbp5*), that we validated by qPCR (Supplementary Fig. S7A). Overexpression of these genes has been reported in several human cancers, including pancreatic cancer (*GATA6*; ref. 33), B-cell chronic lymphocytic leukemia (B-CLL) and follicular lymphoma (*PRKCB*; ref. 34), and liver cancer (*IGFBP5*; ref. 35). Many cancer-related genesets and several oncogenic signatures were enriched in genes upregulated in transformed *Smchd1*-null MEFs and/or tumors, including E2F3 (29 genes, $P < 0.05$), E2F1/E2F (2 genesets, $P < 0.05$), and BRCA1/2 pathways (5 genesets, $P < 0.01$), which may explain the accelerated tumor growth in the absence of Smchd1. Strikingly, target genes of MYC (in human B cells and Burkitt's lymphoma cells, 8 genesets, $P < 0.01$), polycomb-repressive complex 2 (PRC2, in prostate cancer and human embryonic stem cells, 2 genesets, $P < 0.05$), and NIPP1, a transcriptional repressor reported to cooperate with PRC2 (871 genes, $P < 0.05$), were also overrepresented in genes upregulated in transformed *Smchd1*-null MEFs and tumors, suggesting a functional interaction between Smchd1, Myc, and PRC2. Smchd1 and PRC2 may cooperate to silence some targets, as they do on the inactive X chromosome (2).

We conducted the same analyses with Eμ-*Myc*$^{Tg/+}$ samples and observed a similar trend, whereby premalignant pre-B cells exhibited the highest number of differentially expressed genes compared with either E17.5 pre-B cells or end-stage lymphomas (Fig. 4B and Supplementary Fig. S6B). In addition to the 2 imprinted genes, *Ndn* and *Mkrn3*, which were consistently overexpressed, and validated by qPCR (Supplementary Fig. S7B), enrichment of cancer-related genesets was also observed in E17.5 *Smchd1*$^{gt/gt}$/Eμ-*Myc*$^{Tg/+}$ pre-B cells compared with littermate controls, namely B-CLL (59 genes, $P < 0.05$) and multiple myeloma (40 genes, $P < 0.05$; Supplementary Table S4). In premalignant pre-B cells, we found upregulation of proto-oncogenes, *Cyclin D1*, *Fos*, *Jun*, and *Lmo2*, in the absence of Smchd1. Notably, the identification of expression signatures of *MLL* chimeric fusion genes (3 genesets, $P < 0.05$) in *Smchd1*$^{gt/gt}$/Eμ-*Myc*$^{Tg/+}$ pre-B cells raised the possibility that Smchd1 may functionally oppose Mll in *Myc*-driven lymphomas and conversely, loss of *Smchd1* may cooperate with MLL overexpression. *MLL* encodes an H3K4 methyltransferase and is frequently translocated with other proto-oncogenes, for example, AF4 and AF9, in human acute lymphoid and myeloid leukemia (36, 37). Of the 217 genes in the MLL chimeric fusion genesets (38, 39), 54 showed evidence of upregulation in our study, 4 of which were significant at the level of whole-genome testing (*Gpc1*, *Prickle1*, *Capg* and *Lgals1*). These data suggest that Smchd1 may repress a subset of genes required for *Mll*-driven leukemia and that upregulation of these genes in the absence of Smchd1 may contribute to the accelerated formation of lymphomas observed.

Taken together, our data indicate that Smchd1 acts as a tumor suppressor in 2 oncogene-driven models. Smchd1 is

ubiquitously expressed but varies more than 20-fold between cell types (26, 27). As the B-cell lineage shows the highest levels of *Smchd1* expression and MEFs have below median levels, this suggests that abundance of Smchd1 does not determine its function as a tumor suppressor. Rather, at least in this regard, Smchd1 has the potential to act as a tumor suppressor in multiple cell types. In the context of lymphoma, the enhanced clonogenicity of premalignant Eμ-*Myc*$^{Tg/+}$ pro-B cells *in vitro* implicates increased replicative potential as the underlying basis for the elevated pre- B-cell numbers observed *in vivo* in the absence of Smchd1, with an expanded pool of targets for Eμ-*Myc* transformation causing the markedly accelerated disease. Our gene expression analysis revealed the intriguing possibility that Smchd1 normally represses genes in common with those activated by MLL chimeric fusion proteins. This implies that loss of Smchd1 and overexpression of MLL fusion proteins may work through similar pathways in leukemia and lymphoma. Potentially, the genes that drive disease in these cases are common targets of Smchd1 and MLL fusion proteins.

Importantly, mouse *Smchd1* shares 86% sequence identity with its human homolog, and SMCHD1 is similarly ubiquitously expressed in human (26, 27). Although it is not yet known whether SMCHD1 has a role in human cancers, in light of our findings in Myc-driven lymphoma, it is interesting to note that *SMCHD1* is significantly underexpressed in nine classes of human hematopoietic malignancy (including B- and T-cell acute and chronic leukemias, B-cell lymphomas, and one myeloma dataset) across 8 independent datasets when compared with normal bone marrow or peripheral blood samples (40). Downregulation of *SMCHD1* was observed most consistently, across 3 independent datasets, in diffuse large B-cell lymphoma, an aggressive non–Hodgkin B-cell lymphoma. More broadly, LOH of chromosome 18p occurs in 23% of all cancer sample cases on the CONAN database, whereas amplification of 18p occurs in less than 0.3% of cases (734 samples; ref. 41). Indeed, the region containing *SMCHD1* is deleted in more than 30% of cases of colorectal, breast, and lung cancer (41, 42). The most consistent change in *SMCHD1* expression, across all cancers, is greater than 2-fold reduction in expression in colorectal cancer samples compared with normal tissue, seen in 5 independent colorectal cancer datasets (40). These data raise the possibility that SMCHD1 also acts as a tumor suppressor in human malignancy. Interestingly, a recent report has identified heterozygous mutations in *SMCHD1* in fascioscapulohumoral dystrophy type 2; the first reported mutations in *SMCHD1* (43). It will be important to investigate whether these patients may also be cancer prone.

Disclosure of Potential Conflicts of Interest

No potential conflicts of interest were disclosed.

Authors' Contributions

Conception and design: K. Chen, D.J. Hilton, M.E. Blewitt
Development of methodology: H.S. Leong, S. Lee, G.K. Smyth, M.E. Blewitt
Acquisition of data (provided animals, acquired and managed patients, provided facilities, etc.): H.S. Leong, K. Chen, J. Corbin, M. Pakusch, W.S. Alexander, M.E. Blewitt
Analysis and interpretation of data (e.g., statistical analysis, biostatistics, computational analysis): H.S. Leong, Y. Hu, S. Lee, J.M. Murphy, I.J. Majewski, G.K. Smyth, W.S. Alexander, M.E. Blewitt
Writing, review, and/or revision of the manuscript: H.S. Leong, K. Chen, J.M. Murphy, G.K. Smyth, W.S. Alexander, D.J. Hilton, M.E. Blewitt
Administrative, technical, or material support (i.e., reporting or organizing data, constructing databases): H.S. Leong, J. Corbin, M. Pakusch
Study supervision: J.M. Murphy, W.S. Alexander, M.E. Blewitt

Acknowledgments

The authors thank Graham Kay, Ricky Johnstone, Ross Dickins, Sarah Kinkel, Jamie Gearing, and Darcy Butts for helpful discussions and Ross Dickins for constructs.

Grant Support

This work was supported by Fellowships (M.E. Blewitt, I.J. Majewski, G.K. Smyth, W.S. Alexander, and D.J. Hilton) a Program Grant (461219 to W.S. Alexander and D.J. Hilton), and IRIISS support from the Australian National Health and Medical Research Council, Fellowships from the Australian Research Council (M.E. Blewitt and J.M. Murphy), Melbourne University International Research Scholarships (H.S. Leong and K. Chen), an Australian Postgraduate Award (S. Lee), Dyson Bequest funding (M.E. Blewitt), and a Victorian State Government Operational Infrastructure Support Grant.

The costs of publication of this article were defrayed in part by the payment of page charges. This article must therefore be hereby marked *advertisement* in accordance with 18 U.S.C. Section 1734 solely to indicate this fact.

Received August 1, 2012; revised November 28, 2012; accepted December 20, 2012; published OnlineFirst December 26, 2012.

References

1. Blewitt ME, Vickaryous NK, Hemley SJ, Ashe A, Bruxner TJ, Preis JI, et al. An N-ethyl-N-nitrosourea screen for genes involved in variegation in the mouse. Proc Natl Acad Sci U S A 2005;102:7629–34.
2. Blewitt ME, Gendrel AV, Pang Z, Sparrow DB, Whitelaw N, Craig JM, et al. SmcHD1, containing a structural-maintenance-of-chromosomes hinge domain, has a critical role in X inactivation. Nat Genet 2008; 40:663–9.
3. Hirano T. At the heart of the chromosome: SMC proteins in action. Nat Rev Mol Cell Biol 2006;7:311–22.
4. Kanwal R, Gupta S. Epigenetic modifications in cancer. Clin Genet 2012;81:303–11.
5. Adams JM, Harris AW, Pinkert CA, Corcoran LM, Alexander WS, Cory S, et al. The c-myc oncogene driven by immunoglobulin enhancers induces lymphoid malignancy in transgenic mice. Nature 1985; 318:533–8.
6. Egle A, Harris AW, Bouillet P, Cory S. Bim is a suppressor of Myc-induced mouse B cell leukemia. Proc Natl Acad Sci U S A 2004;101: 6164–9.
7. Majewski IJ, Blewitt ME, de Graaf CA, McManus EJ, Bahlo M, Hilton AA, et al. Polycomb repressive complex 2 (PRC2) restricts hematopoietic stem cell activity. PLoS Biol 2008;6:e93.
8. Serrano M, Lin AW, McCurrach ME, Beach D, Lowe SW. Oncogenic ras provokes premature cell senescence associated with accumulation of p53 and p16INK4a. Cell 1997;88:593–602.
9. Dickins RA, Hemann MT, Zilfou JT, Simpson DR, Ibarra I, Hannon GJ, et al. Probing tumor phenotypes using stable and regulated synthetic microRNA precursors. Nat Genet 2005;37:1289–95.
10. Ripoll GV, Giron S, Krzymuski MJ, Hermo GA, Gomez DE, Alonso DF. Antitumor effects of desmopressin in combination with chemotherapeutic agents in a mouse model of breast cancer. Anticancer Res 2008;28:2607–11.
11. Vert JP, Foveau N, Lajaunie C, Vandenbrouck Y. An accurate and interpretable model for siRNA efficacy prediction. BMC Bioinformatics 2006;7:520.
12. DSIR France: CEA; 2007 [updated 2009 Jul 28; cited 2008 Jun 1]. Available from: http://biodev.cea.fr/DSIR/DSIR.html.

13. Gentleman RC, Carey VJ, Bates DM, Bolstad B, Dettling M, Dudoit S, et al. Bioconductor: open software development for computational biology and bioinformatics. Genome Biol 2004;5:R80.
14. Shi W, Oshlack A, Smyth GK. Optimizing the noise versus bias trade-off for Illumina whole genome expression BeadChips. Nucleic Acids Res 2010;38:e204.
15. Smyth GK. Linear models and empirical bayes methods for assessing differential expression in microarray experiments. Stat Appl Genet Mol Biol 2004;3:Article3.
16. Ritchie ME, Diyagama D, Neilson J, van Laar R, Dobrovic A, Holloway A, et al. Empirical array quality weights in the analysis of microarray data. BMC Bioinformatics 2006;7:261.
17. Smyth GK, Michaud J, Scott HS. Use of within-array replicate spots for assessing differential expression in microarray experiments. Bioinformatics 2005;21:2067–75.
18. Benjamini Y, Hochberg Y. Controlling the false discovery rate: a practical and powerful approach to multiple testing. J Roy Stat Soc Ser B 1995;57:289–300.
19. Wu D, Smyth GK. Camera: a competitive gene set test accounting for inter-gene correlation. Nucleic Acids Res 2012;40:e133.
20. Subramanian A, Tamayo P, Mootha VK, Mukherjee S, Ebert BL, Gillette MA, et al. Gene set enrichment analysis: a knowledge-based approach for interpreting genome-wide expression profiles. Proc Natl Acad Sci U S A 2005;102:15545–50.
21. Jackson Laboratory Mammalian Orthology Tables [Internet]. The Jackson Laboratory. [cited 2012 Mar 8]. Available from: https://http://www.informatics.jax.org/orthology.shtml.
22. WEHI bioinformatics MSigDB software Melbourne: Walter and Eliza hall institute bioinformatics division; [cited 2012 Mar 8]. Available from: http://bioinf.wehi.edu.au/software.MSigDB.
23. WEHI bioinformatics compare curves software Melbourne: Walter and Eliza hall institute bioinformatics division; [cited 2009 Sept 1]. Available from: http://bioinf.wehi.edu.au/software/compareCurves/.
24. Elso CM, Roberts LJ, Smyth GK, Thomson RJ, Baldwin TM, Foote SJ, et al. Leishmaniasis host response loci (lmr1-3) modify disease severity through a Th1/Th2-independent pathway. Genes Immun 2004;5:93–100.
25. Hu Y, Smyth GK. ELDA: extreme limiting dilution analysis for comparing depleted and enriched populations in stem cell and other assays. J Immunol Methods 2009;347:70–8.
26. Wu C, Orozco C, Boyer J, Leglise M, Goodale J, Batalov S, et al. BioGPS: an extensible and customizable portal for querying and organizing gene annotation resources. Genome Biol 2009;10:R130.
27. BioGPS [Internet]. Scripps Research Institute. [cited 2012 June 1]. Available from: http://biogps.gnf.org.
28. Langdon WY, Harris AW, Cory S, Adams JM. The c-myc oncogene perturbs B lymphocyte development in E-mu-myc transgenic mice. Cell 1986;47:11–8.
29. Held W, Roland J, Raulet DH. Allelic exclusion of Ly49-family genes encoding class I MHC-specific receptors on NK cells. Nature 1995;376:355–8.
30. Esumi S, Kakazu N, Taguchi Y, Hirayama T, Sasaki A, Hirabayashi T, et al. Monoallelic yet combinatorial expression of variable exons of the protocadherin-alpha gene cluster in single neurons. Nat Genet 2005;37:171–6.
31. Taniura H, Taniguchi N, Hara M, Yoshikawa K. Necdin, a postmitotic neuron-specific growth suppressor, interacts with viral transforming proteins and cellular transcription factor E2F1. J Biol Chem 1998;273:720–8.
32. Taniura H, Matsumoto K, Yoshikawa K. Physical and functional interactions of neuronal growth suppressor necdin with p53. J Biol Chem 1999;274:16242–8.
33. Fu B, Luo M, Lakkur S, Lucito R, Iacobuzio-Donahue CA. Frequent genomic copy number gain and overexpression of GATA-6 in pancreatic carcinoma. Cancer Biol Ther 2008;7:1593–601.
34. Li S, Phong M, Lahn M, Brail L, Sutton S, Lin BK, et al. Retrospective analysis of protein kinase C-beta (PKC-beta) expression in lymphoid malignancies and its association with survival in diffuse large B-cell lymphomas. Biol Direct 2007;2:8.
35. Umemura A, Itoh Y, Itoh K, Yamaguchi K, Nakajima T, Higashitsuji H, et al. Association of gankyrin protein expression with early clinical stages and insulin-like growth factor-binding protein 5 expression in human hepatocellular carcinoma. Hepatology 2008;47:493–502.
36. Gu Y, Nakamura T, Alder H, Prasad R, Canaani O, Cimino G, et al. The t(4;11) chromosome translocation of human acute leukemias fuses the ALL-1 gene, related to Drosophila trithorax, to the AF-4 gene. Cell 1992;71:701–8.
37. Nakamura T, Alder H, Gu Y, Prasad R, Canaani O, Kamada N, et al. Genes on chromosomes 4, 9, and 19 involved in 11q23 abnormalities in acute leukemia share sequence homology and/or common motifs. Proc Natl Acad Sci U S A 1993;90:4631–5.
38. Ross ME, Mahfouz R, Onciu M, Liu HC, Zhou X, Song G, et al. Gene expression profiling of pediatric acute myelogenous leukemia. Blood 2004;104:3679–87.
39. Gaussmann A, Wenger T, Eberle I, Bursen A, Bracharz S, Herr I, et al. Combined effects of the two reciprocal t(4;11) fusion proteins MLL.AF4 and AF4.MLL confer resistance to apoptosis, cell cycling capacity and growth transformation. Oncogene 2007;26:3352–63.
40. Oncomine.org [Internet]. Compendia Bioscience C2008–2012. [cited 2012 July 31]. Available from: http://www.oncomine.org.
41. CONAN: Copy number analysis [Internet]. Welcome Trust Sanger Institute. [cited 2012 July 31]. Available from: http://www.sanger.ac.uk/cgi-bin/genetics/CGP/conan/search.cgi.
42. The Cancer Genome Atlas [Internet]. National Cancer Institute and National Genome Research Institute. [cited 2012 Jul 31]. Available from: http://cancergenome.nih.gov/.
43. Lemmers RJ, Tawil R, Petek LM, Balog J, Block GJ, Santen GW, et al. Digenic inheritance of an SMCHD1 mutation and an FSHD-permissive D4Z4 allele causes facioscapulohumeral muscular dystrophy type 2. Nat Genet 2012;44:1370–4.